

RESEARCH ARTICLE

Quantifying progression in primary progressive aphasia with structural neuroimaging

Jolina Lombardi¹ | Benjamin Mayer² | Elisa Semler¹ | Sarah Anderl-Straub¹ | Ingo Uttner¹ | Jan Kassubek¹ | Janine Diehl-Schmid^{3,6} | Adrian Danek⁴ | Johannes Levin^{4,5,6} | Klaus Fassbender⁷ | Klaus Fliessbach^{8,9} | Anja Schneider^{8,9} | Hans-Jürgen Huppertz¹⁰ | Holger Jahn¹¹ | Alexander Volk¹² | Johannes Kornhuber¹³ | Bernhard Landwehrmeyer¹ | Martin Lauer¹⁴ | Johannes Prudlo^{15,16} | Jens Wiltfang¹⁷ | Matthias L. Schroeter¹⁸ | Albert Ludolph¹ | Markus Otto¹ | the FTLD consortium*

¹ Department of Neurology, University Hospital Ulm, Ulm, Germany

² Institute for Epidemiology and Medical Biometry, University of Ulm, Ulm, Germany

³ Department of Psychiatry and Psychotherapy, Technical University of Munich, Munich, Germany

⁴ Department of Neurology, Ludwig-Maximilians-Universität München, Munich, Germany

⁵ German Center for Neurodegenerative Diseases (DZNE), Munich, Germany

⁶ Munich Cluster for Systems Neurology (SyNergy), Munich, Germany

⁷ Department of Neurology, Saarland University Hospital, Homburg, Germany

⁸ Department of Psychiatry and Psychotherapy, University Hospital Bonn, Bonn, Germany

⁹ German Center for Neurodegenerative Diseases (DZNE), Bonn, Germany

¹⁰ Swiss Epilepsy Center, Zurich, Switzerland

¹¹ Department of Psychiatry and Psychotherapy, University Hospital Hamburg Eppendorf, Hamburg, Germany

¹² Institute for Human Genetics, University Hospital Hamburg Eppendorf, Hamburg, Germany

¹³ Department of Psychiatry and Psychotherapy, University Hospital Erlangen, Erlangen, Germany

¹⁴ Department of Psychiatry and Psychotherapy, University Hospital Würzburg, Würzburg, Germany

¹⁵ Department of Neurology, University Medicine Rostock, Rostock, Germany

¹⁶ German Center for Neurodegenerative Diseases (DZNE), Rostock, Germany

¹⁷ Department of Psychiatry and Psychotherapy, Medical University Göttingen, Göttingen, Germany

¹⁸ Max-Planck-Institute for Human Cognitive and Brain Sciences and Clinic for Cognitive Neurology, University Hospital Leipzig, Leipzig, Germany

Correspondence

Markus Otto, Professor for Neurology, Department of Neurology, University of Ulm, Oberer Eselsberg 45, 89081 Ulm, Germany.
E-mail: markus.otto@uni-ulm.de

* FTLD consortium: Christine von Arnim, Petra Steinacker, Hans-Peter Müller, Felix Oberhauser, Kai Schumacher, Jan Lehmebeck, Juan-Manuel Maler, Tanja Richter-Schmidinger, Anke Hammer-Kaspereit, Timo Oberstein, Daniele Pino, Maryna Polyakova, Lea Hüper, Frank Regenbrecht, Angelika Thöne-Otto, Felix Müller-Sarnowski, Carola Roßmeier.

Abstract

Introduction: The term primary progressive aphasia (PPA) sums up the non-fluent (nfv), the semantic (sv), and the logopenic (lv) variant. Up to now, there is only limited data available concerning magnetic resonance imaging volumetry to monitor disease progression.

Methods: Structural brain imaging and an extensive assessment were applied at baseline and up to 4-year(s) follow-up in 269 participants. With automated atlas-based volumetry 56 brain regions were assessed. Atrophy progression served to calculate sample sizes for therapeutic trials.

Funding information

German Federal Ministry of Education and Research, Grant/Award Number: FKZ01GI1007A; EU Joint Programme—Neurodegenerative Disease Research, Grant/Award Number: 01ED1512; Baden-Württemberg, Grant/Award Numbers: D.3830, D.5009; German Research Foundation, Grant/Award Number: SCHR 774/5-1; German Federal Ministry of Education and Research, Grant/Award Number: FKZ01GI1007A; EU Joint Programme—Neurodegenerative Disease Research, Grant/Award Number: 01ED1512; Baden-Württemberg, Grant/Award Numbers: D.3830, D.5009; German Research Foundation, Grant/Award Number: SCHR 774/5-1

Results: At baseline highest atrophy appeared in parts of the left frontal lobe for nfvPPA (−17%) and of the left temporal lobe for svPPA (−34%) and lvPPA (−24%). Severest progression within 1-year follow-up occurred in the basal ganglia in nfvPPA (−7%), in the hippocampus/amygdala in svPPA (−9%), and in (medial) temporal regions in lvPPA (−6%).

Conclusion: PPA presents as a left-dominant, mostly gray matter sensitive disease with considerable atrophy at baseline that proceeds variant-specific.

KEYWORDS

atlas-based volumetry, disease progression, frontotemporal dementia, longitudinal magnetic resonance imaging, primary progressive aphasia, sample size calculation

1 | INTRODUCTION

Primary progressive aphasia (PPA) is defined as a gradually developing, progressive language impairment that is the most salient deficit during early stages of the disease and has no other cause than neurodegenerative processes.¹ Three main subtypes have been defined, that is, the non-fluent (nfvPPA), the semantic (svPPA), and the logopenic (lvPPA) variants.² Each subtype presents with a particular clinical phenotype. NfvPPA is characterized by a slow, effortful speech with inconsistent sound errors; grammatical failures; fragmented, telegram-like sentences; and an impaired comprehension of more complex instructions.^{2,3} SvPPA often manifests with naming impairments, impeded single word comprehension, surface dyslexia or dysgraphia, and decreased object knowledge.^{1,2} LvPPA includes impaired word retrieval, phonological errors in spontaneous speech and naming, as well as hampered repetition of sentences that is supposed to be a consequence of verbal short-term memory deficits primarily.^{2,4,5} Imaging biomarkers support classification and are especially important to track clinico-anatomical correlates as each subgroup is associated with regionally selective neuronal loss.⁶ In fact, PPA variants can be separated both from healthy controls and from one another with structural measurements.⁷ The hallmark of PPA is a cerebral atrophy in regions involved in language processing with a focus on the inferior frontal gyrus and the insula cortex with extension to the superior temporal gyrus in nfvPPA, the anteroinferior temporal lobe in svPPA, and the posterior superior temporal and inferior parietal cortices in lvPPA.^{4,8–11} Accordingly, atrophy is dominantly left lateralized within the (asymmetrically organized) language network, disease-specific (at least in the beginning of the condition), and differs in progression rate between subtypes.^{8,12–18} In the course of the disease, however, additional symptoms may occur and clinical syndromes finally blur.^{1,19,20}

There is only limited data available concerning longitudinal magnetic resonance imaging (MRI) volumetry as an objective parameter to monitor disease progression and to calculate sample sizes for disease-modifying therapeutic trials. So far, studies reported annual changes in whole brain volume (WBV) in PPA subgroups ranging from −1.6% to −2.9% (n = 9 to 21),^{15–17,21–24} whereas in healthy maturation an annual

WBV loss of about 0.5% (n = 142) is supposed to start at age 30 and accumulating with age.^{25–27} Sample sizes to detect a therapeutic effect of 25% (40%) ranged from n = 135 to 158 (n = 54 to 62) for svPPA, n = 105 to 777 (n = 42–303) for nfvPPA, and n = 81 (n = 32) for lvPPA.^{23,28}

To entangle structural MRI data by examining brain atrophy evidence-based and without a priori defined regions to monitor disease progression we address the following hypotheses: (1) All PPA subtypes should present at baseline with disease-specific atrophy patterns that differ from healthy controls and from each other.^{7,8} (2) Disease progression is related to increasing and more widespread atrophy. (3) Atrophy rates within and between groups define most vulnerable regions and enable calculation of reliable sample sizes for therapeutic trials. (4) Sample sizes are calculated for progression over 1- and 2-year follow-up comparing their respective statistical power.

2 | METHODS**2.1 | Study population**

With data-lock in 2018, n = 269 participants from the German Frontotemporal Lobar Degeneration (FTLD) consortium sample with at least one and up to four visits with MRI scan were either included and evaluated as healthy control (CON) or diagnosed with PPA according to the valid criteria.² After exclusion of inchoate data and demographic outliers, n = 95 participants (CON n = 25, nfvPPA n = 29, svPPA n = 22, lvPPA n = 19) completed a baseline (V1) and a consecutive 1-year follow-up (V2) examination, and of those n = 43 a 2-year follow-up (V3) visit. To increase sample size for longitudinal disease tracking we included a further n = 11 subjects (CON n = 2, nfvPPA n = 3, svPPA n = 5, lvPPA n = 1) that passed the baseline (V1) and the 2-year follow-up (V3) examination (missing the V2). A total of n = 106 subjects and their volumetric data of up to three timepoints (V1 to V3) was finally included in this study. Data were collected between 2011 and 2018 from 10 German sites (Bonn, Erlangen, Göttingen, Hamburg, Homburg/Saar, Leipzig, Munich, Rostock, Ulm, Würzburg); data subsets have been used previously.^{29,30}

HIGHLIGHTS

- Early on, PPA variants show distinct atrophy patterns
- Frontal areas and subcortical basal ganglia are particularly affected in nfvPPA
- Atrophy and its longitudinal progression is locally most restricted in svPPA
- Profound volume loss in lvPPA includes frontal, temporal and parietal regions
- Therapeutic trials can be based on at least 30 patients per group

RESEARCH IN CONTEXT

1. **Systematic review:** The authors reviewed the existing literature concerning progression markers, location, and quantification of atrophy in primary progressive aphasia (PPA). Although clinical phenotypes have been described in detail, magnetic resonance imaging volumetry as an objective parameter to monitor disease progression is still limited.
2. **Interpretation:** Our findings provide detailed information of longitudinal pathologic brain volume decrease without a priori defined regions in all three defined PPA subtypes.
3. **Future directions:** The longitudinal subtype-specific analysis of disease progression allows us to comprehend primary and secondary affected brain regions and thus appropriate sites to evaluate therapeutic trials. However, further research needs to (1) clarify individual disease progression in terms of predictive models; (2) elaborate criteria that are capable of accommodating additional, mixed, or unclassifiable symptoms that may occur in early or late stages of the disease taking into account clinico-anatomical correlates; (3) work out spotting the earliest possible pathologic alterations to implement best therapeutic interventions.

2.2 | Genetic testing

Genetic testing for most causative gene mutations in FTLD (*C9orf72*, *MAPT*, *GRN*, *TBK1*) confirmed a total of six pathogenic mutation carriers among the patient group (Table 1).

2.3 | Neuropsychological and clinical assessment

Each study visit included a neurological and an extensive neuropsychological protocol (for details see Semler et al.²⁹) The balanced PPA

sum score²⁹ indicated each patient's language abilities. Trained raters conducted the Frontotemporal-specific Clinical Dementia Rating Scale (FTLD-CDR)³¹ at each visit.

2.4 | Neurochemical markers

At baseline visit, cerebrospinal fluid (CSF) was taken to determine tau, phosphorylated tau (p-tau), and amyloid beta (A β). Blood samples were collected to measure neurofilament light chain levels (NFL)³⁰ at each visit (Table 1).

2.5 | Imaging data acquisition and volumetric analysis

For diagnostic purposes, patients received an FDG- and amyloid-PET at baseline visit, if available. All imaging data were collected in accordance with the standard operating procedures (SOPs) of the FTLD consortium. A 3 Tesla MRI scan was conducted at baseline and every year follow-up (layer thickness: 1 mm, repetition time: 2300 milliseconds, echo time: 3.0 milliseconds, inversion time: 900 milliseconds, voxel x/y/z: 1/1/1mm). In preparation, the T1-weighted magnetization-prepared rapid gradient echo (MPRAGE) sequence image of each MRI underwent a thorough quality control by sight and was converted from Digital Imaging and Communications in Medicine (DICOM) format into Neuroimaging Informatics Technology Initiative (NIfTI) file format with the help of the MRICConvert program (version 2.0 rev.235, Lewis Center for Neuroimaging, University of Oregon; <http://lcn.uoregon.edu>). Images were then processed and analyzed for 56 target regions defined by the LONI Probabilistic Brain Atlas (LPBA40) including 50 cortical structures, four subcortical areas, brainstem, and cerebellum³² with the help of fully automated atlas-based volumetry (ABV)³³ that allows a further subdivision into gray and white matter (for detailed procedure see Appendix S1 in supporting information).

2.6 | Statistical analysis

Statistical analyses were performed with IBM SPSS Statistics for Windows, Version 25, and R software, Version 3.6.1.

2.6.1 | Cross-sectional data

Normal distribution was examined with the Shapiro-Wilk test (or Kolmogorov-Smirnoff test for ordinal data). Differences in central tendencies between groups in demographic data, clinical, and cognitive results were conducted either with a univariate analysis of variance with Bonferroni or Dunnett-T3 post hoc test or with a Kruskal-Wallis H test and Bonferroni correction for ordinal data and in case of non-parametrical distributions. To make volumetric data between groups comparable and to control for effects of disparate head sizes, results

TABLE 1 Demographic data for study population

		CON		NfvPPA		SvPPA		lvPPA	
		N	Mean (±SD)	N	Mean (±SD)	N	Mean (±SD)	N	Mean (±SD)
V1 (baseline) N	106	27		32		27		20	
Demographics									
Sex [f:m]		27	11:16	32	16:16	27	12:15	20	11:9
Handedness [right/mixed/left]		27	26/1/-	32	27/-/5	27	32/-/-	20	15/2/3
Age at symptom onset (years)		-	-	32	65.2 (±8.9)** ^c	26	58.5 (±7.7)	20	63.5 (±6.3)
Age at baseline (years)		27	68.1 (±8.3)	32	67.8 (±8.6)	27	62.9 (±7.2) ^{†d}	20	69.1 (±5.1)
Education (years)		26	14.7 (±2.9)	31	13.1 (±3.4)	24	14.5 (±3.3)	20	12.8 (±3.2)
Disease duration (years)		-	-	32	2.1 (±1.7) ^{†d}	26	3.3 (±2.5)	20	4.5 (±3.2)
Neurochemical markers									
Tau (CSF)		-	-	26	355.4 (±157.4)	17	486.6 (±338.5)	14	588.3 (±433.3)
pTau (CSF)		-	-	24	51.6 (±26.6)	16	59.4 (±29.2)	12	80.1 (±57.8)
Aβ42 (CSF)		-	-	27	994.9 (±324.0)** ^d	17	871.0 (±435.3)	15	612.7 (±306.3)
NfL (serum)		11	17.3 (±15.8)	23	38.3 (±20.7)** ^a	22	28.0 (±12.4) ^a	15	23.3 (±13.6)
Neuropsychology & clinical rating									
MMSE		27	29.2 (±0.8)*** ^{b,c,d}	31	23.8 (±5.6)	26	23.7 (±5.9)	20	21.8 (±6.3)
CDR		25	0.0 (±0.1)*** ^{b,c,d}	28	2.2 (±2.6)	25	3.1 (±2.3)	18	3.2 (±3.1)
FTLD-CDR		25	0.0 (±0.1)*** ^{b,c,d}	28	4.3 (±3.4)	25	5.0 (±3.0)	18	4.9 (±3.8)
PPA-sum score (balanced) ²⁶		13	334.4 (±11.7)*** ^{b,c,d}	19	245.1 (±48.1)	16	246.0 (±44.5)	13	254.5 (±43.4)
Neuroimaging									
MRI		27		32		17		20	
FDG-PET		2		26		18		15	
Genetic testing		15		26		25		17	
C9orf72/GRN/MAPT/TBK1		-		3		2		1	
V2 (1-year follow-up) N	94	24		29		22		19	
Demographics									
Sex [f:m]		24	10:14	29	13:16	22	11:11	19	10:9
Age (years)		24	69.3 (±8.7)	29	68.8 (±8.6)	22	63.8 (±7.9)	19	70.2 (±5.3)
Neurochemical markers									
NfL (serum)		12	13.3 (±4.5)*** ^{b,c}	19	47.2 (±32.9)	18	36.5 (±15.9)	14	24.0 (±13.4)
Neuropsychology & clinical rating									
MMSE		23	28.9 (±1.0)*** ^{b,c,d}	27	21.1 (±7.4)	21	20.5 (±8.9)	18	19.2 (±8.7)
CDR		20	0.1 (±0.2)*** ^{b,c,d}	25	3.5 (±3.4)	21	5.1 (±3.2)	16	4.8 (±3.9)
FTLD-CDR		20	0.1 (±0.2)*** ^{b,c,d}	25	6.4 (±4.4)	21	7.8 (±4.3)	16	7.3 (±4.6)
PPA-sum score (balanced)		14	335.5 (±9.1)*** ^{b,c,d}	18	222.1 (±61.1)	15	228.3 (±46.9)	11	243.0 (±36.0)
V3 (2-year follow-up) N	54	12		18		15		9	
Demographics									
Sex [f:m]		12	4:8	18	11:7	15	3:12	9	6:3
Age (years)		12	69.8 (±7.9)	18	69.8 (±7.9)	15	63.1 (±7.1)	9	71.0 (±5.4)

(Continues)

TABLE 1 (Continued)

	CON		NfvPPA		SvPPA		lvPPA	
	N	Mean (±SD)	N	Mean (±SD)	N	Mean (±SD)	N	Mean (±SD)
Neurochemical markers								
NfL (serum)	1	-	10	58.9 (±25.6)	10	40.1 (±29.1)	6	24.4 (±13.9)
Neuropsychology & clinical rating								
MMSE	12	28.7 (±1.0) ^{*,c,d}	13	17.0 (±10.1) ^{***,a}	11	20.6 (±8.6)	7	18.6 (±7.0)
CDR	12	0.0 (±0.1) ^{***,b,c,d}	15	4.7 (±4.1)	13	5.4 (±4.6)	9	3.8 (±2.3)
FTLD-CDR	12	0.1 (±0.2) ^{***,b,c}	15	8.1 (±4.7)	13	8.4 (±5.8)	9	6.3 (±2.9) ^{*,a}
PPA-sum score (balanced)	7	333.0 (±14.3) ^{*,c,d}	5	163.5 (±83.8) ^{*,a}	7	211.3 (±21.9)	6	202.7 (±81.1)

Abbreviations: CDR, Clinical Dementia Rating; CON, healthy controls; f, female; FTLD-CDR, Frontotemporal-specific Clinical Dementia Rating; lvPPA, logopenic variant primary progressive aphasia; m, male; MMSE, Mini-Mental State Examination; nfvPPA, non-fluent variant of primary progressive aphasia; SD, standard deviation; svPPA, semantic variant of primary progressive aphasia.

Note: Subjects with at least two subsequent visits that were included in cross-sectional and longitudinal data evaluations (n=106). *, *P* <.05; **, *P* <.01; ***, *P* ≤.001.

^aDiffers from CON.

^bDiffers from nfvPPA.

^cDiffers from svPPA.

^dDiffers from lvPPA (cross-sectional comparison).

of the ABV for V1 were corrected for intracranial volume (ICV): Structural volumes per subject were divided by the individual ICV and multiplied with the mean ICV of the whole study population (M[V1] = 1405 mL). Cross-sectional volume disparities between each PPA group and healthy controls were calculated as difference of mean structural volume for each brain region measured by the LPBA40 separately using a simply contrasted analysis of covariance (ANCOVA) with factor group and the covariates age and sex. The level of significance was set to *P* = .05. Because the analysis approach was fully explorative, adjustment of results due to multiple testing was not performed. Only volume disparities *P* <.001 were reported.

2.6.2 | Longitudinal data

Longitudinal MRI measurements (for three timepoints, V1 to V3) were analyzed by means of R software (www.r-project.org). To correct for chronological interval, volumetric data of follow-up appointment was corrected and consistently set 365 days (730 days in case V2 was missing) after the previous visit. Therefore, volume difference between visits was divided by the exact count of days between baseline and the consecutive 1-year (2-year) follow-up measurement and multiplied with the factor 365 (730, respectively). The corrected annual volume decline was deducted from the baseline volume. To analyze the data descriptively, patient-individual trajectories and box and whisker plots separated by disease group were created initially. Longitudinal measures were then assessed in two ways: First, volume information of each PPA group was compared to healthy controls. A possible impact of disease group and time point of visit on MRI measurements, adjusted for age at baseline and sex, had been investigated using a linear mixed-effects (LME) model ("lmerTest" package)³⁴ using annualized data of the first three visits. Results from the LME model with *P* <.001 were

reported. Second, the course of volume change was retraced within each group to describe variant-specific atrophy progression over time. To control for possible confounding factors (e.g., disease duration, age at symptom onset, handedness, bias between centers) sensitivity analyses were performed (Appendix S2 in supporting information).

2.6.3 | Sample size estimation

The annualized volume decline (for 1- and 2-year disease progression) in percent per subject per group served to generate sample size estimates: First, standardized effect sizes based on mean volume differences between patients and healthy controls were computed (for detailed procedure see Müller et al.³⁵) Then, a theoretical treatment effect of 50%, 20%, and 10% was assumed for all PPA groups separately. Calculation of the minimum sample sizes per group was based on an independent *t*-test assuming a two-sided, explorative type 1 error level of 5% and a statistical power of 80%. A non-parametric bootstrapping approach was used to provide 95% confidence intervals for the estimated sample sizes. Based on 1000 replicates for each scenario, the adjusted bootstrap percentile interval was calculated ("boot" package).

3 | RESULTS

3.1 | Demographics

Table 1 summarizes demographic data, clinical results, and cognitive scores for the eventual study population (n = 106). Sex distribution and years of education showed no substantial difference between groups. Patients with svPPA were younger than those with nfvPPA in relation to age at symptom onset (*P* = .006) and younger than those with lvPPA

concerning age at baseline examination ($P = .043$). In nvPPA disease duration was indicated shorter than in lvPPA ($P = .024$). All PPA subgroups differed from healthy controls ($P < .001$) but not between each other relating to CDR, FTLD-CDR, Mini-Mental State Examination (MMSE), and PPA sum score. The exemplary boxplots and spaghetti plots (Figure 1 and 2) outline the course of brain volume per region over time. For depiction of the whole study population ($n = 269$) see Appendix S1 and S2.

3.2 | Atrophy pattern at baseline

At baseline, brain volume differed significantly between healthy controls and PPA subgroups (Figure 3; Appendix S3 in supporting information). The one-way ANCOVA with planned contrasts revealed that in nvPPA atrophy was most pronounced ($P < .001$) in both frontal lobes, the left temporal, and the left parietal lobe. More specifically, in the bilateral superior (gray matter [GM], white matter [WM]), middle (GM, WM) and inferior (GM, WM) frontal gyrus, the left precentral (GM) gyrus[†], left superior (GM), and middle (GM) temporal gyrus and left angular (WM) gyrus. Beyond that, the left striatum, putamen[†], and hippocampus/amygdala complex[†] delineated as most extensively declined. Atrophy in svPPA compromised most extensively ($P < .001$) both temporal lobes and the left frontal lobe. Primarily, GM volume loss was found in the bilateral superior, middle, and inferior temporal and parahippocampal (right[†]) gyrus while WM decrease appeared in those regions only left lateralized (superior temporal gyrus WM[†]). Also, the left fusiform gyrus (GM, WM), left cingulate gyrus (GM), left insula, left gyrus rectus (GM)[†], left middle frontal gyrus (GM)[†], as well as the left middle (GM)[†] and lateral (GM)[†] orbitofrontal gyrus was contracted. Subcortical structures showed distinct atrophy bilaterally (left > right). Atrophy in patients with lvPPA appeared more widespread with parts of the left frontal, temporal, and parietal lobe notably altered ($P < .001$). Substantial atrophy displayed in the left superior (GM) and middle (GM, WM[†]) frontal gyrus, the left superior (GM, WM[†]), middle (GM, WM) and inferior (GM, WM) temporal gyrus as well as in the left fusiform gyrus (GM), left parahippocampal gyrus (WM[†]), and left insula[†]. Moreover, in the left supramarginal gyrus (GM), left angular gyrus (GM), left precuneus (GM), and left middle occipital gyrus (GM) and also the left striatum[†], putamen, and hippocampus/amygdala complex.

The interaction group \times age reached significance for the hippocampus/amygdala complex ($P = .045$) and the left precuneus WM ($P = .016$), the interaction group \times sex for the parietal lobe WM ($P = .019$; WM_R: $P = .011$) as well as the right supramarginal ($P = .011$) and right postcentral gyrus WM ($P = .044$). After adjustment for multiple comparisons (Bonferroni corrected), single results ([†]) differed slightly from $P < .001$, however all within $P \leq .004$.

A paired *t*-test within each group stated that overall GM decrease was more pronounced than overall WM decline in svPPA ($P = .005$) and lvPPA ($P = .045$) but not in nvPPA.

3.3 | Atrophy progression

Healthy controls showed atrophy rates in distinct regions from 0% to -3% within 1-year follow-up and from 0% to -6% within 2-year follow-up. Comparing overall gray versus white matter atrophy within each PPA group assessed with a paired *t*-test (or Wilcoxon signed-rank test), yielded stronger GM atrophy in svPPA ($P = .009$) within 2-year follow-up, and in lvPPA ($P = .024$) within 1-year follow-up but not in nvPPA.

3.3.1 | Atrophy progression in nvPPA

Compared to healthy controls, notable volume deviation ($P < .001$) appeared over 1-year follow-up in the bilateral superior (GM, WM), middle (GM, WM) and inferior (GM, WM) frontal and precentral gyrus (GM), the superior temporal gyrus (GM), the insula, the supramarginal (GM), and the middle occipital gyrus (GM). Left lateralized volume disparities were located in the middle (GM) and lateral (GM) orbitofrontal gyrus; the middle (GM, WM) and inferior (GM, WM) temporal gyrus; the fusiform (GM), cingulate (GM), postcentral (GM) and angular gyrus (GM, WM); and precuneus (GM). Subcortically, the bilateral striatum, caudate, putamen, and hippocampus/amygdala complex displayed notably reduced volume. Within 2-year follow-up, the left fusiform gyrus (WM), left supramarginal gyrus (WM), and left precuneus (WM) were additionally detected.

Volume decline within the group stated that in nvPPA highest progression rates within 1 year occurred in the left basal ganglia (-7%) and parts of the (left > right) frontal lobe (-5% to -6%; (Figure 4A; Appendix S4 in supporting information). Volumetric changes after 2 years highlighted the same structures (basal ganglia -12%, frontal parts -10%) as most afflicted (Figure 4B; Appendix S4).

3.3.2 | Atrophy progression in svPPA

Compared to healthy controls over both 1- and 2-year follow-up, the LME model revealed that patients with svPPA differed most ($P < .001$) in the bilateral superior (GM, WM_L), middle (GM, WM_L), and inferior (GM, WM) temporal gyrus, as well as in volume of the parahippocampal (GM, WM_L), fusiform (GM, WM_L), and left cingulate (GM) gyrus and bilateral insula. The left superior (GM), middle (GM) and inferior (GM) frontal gyrus, the middle (GM) and lateral (GM) orbitofrontal gyrus, the gyrus rectus (GM), and the angular gyrus (GM) manifested left-lateralized. Moreover, the bilateral striatum, putamen, hippocampus/amygdala complex, and the left caudate deviated significantly.

Within-group volume decline over 1-year follow-up proceeded mainly in the left hippocampus/amygdala complex (-9%) and the left middle and inferior temporal gyrus (-8%) (Figure 4A; Appendix S4). Observing volume change in 2-year follow-up, especially these foci remained most vulnerable with peak atrophy scores of -15% (Figure 4B; Appendix S4).

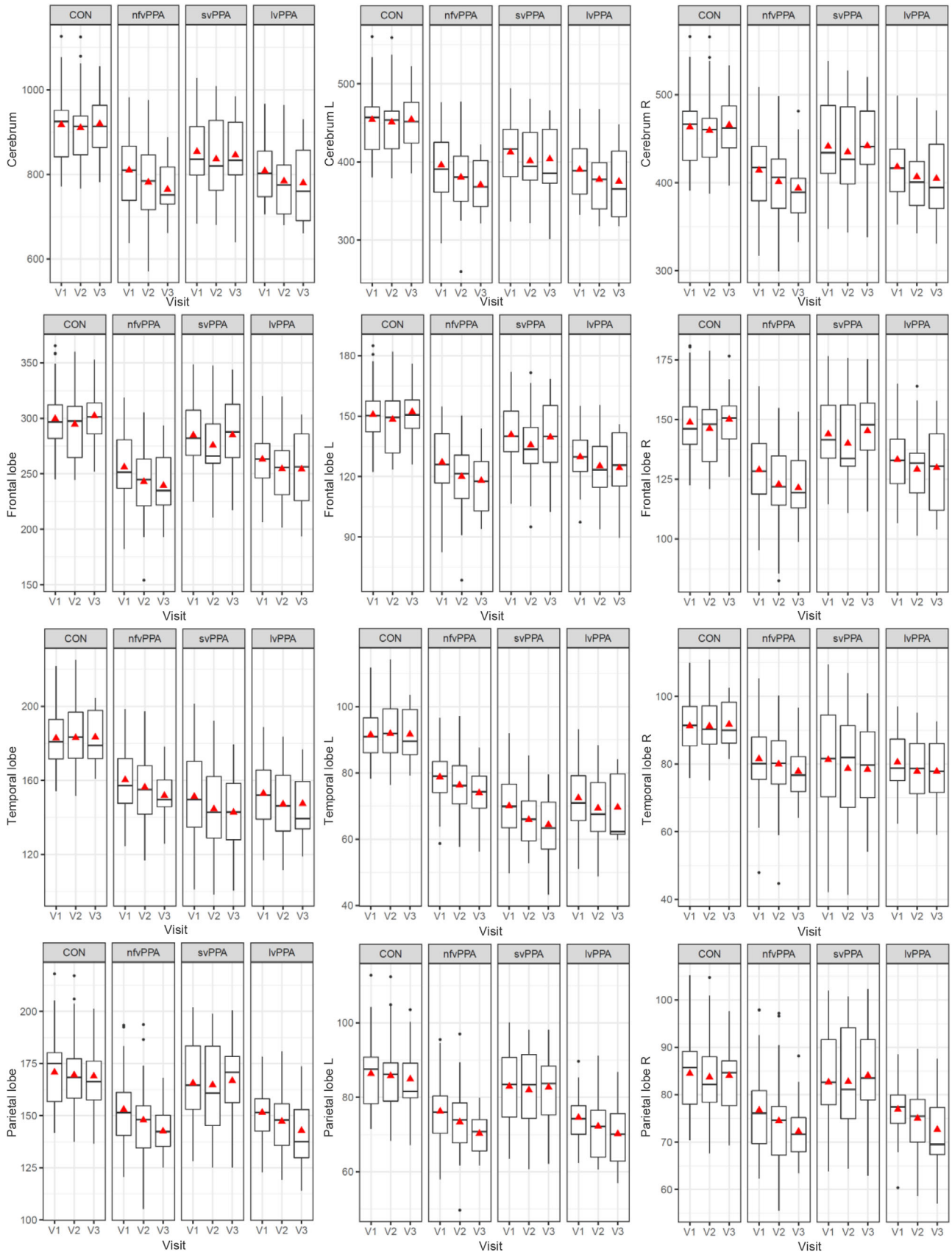


FIGURE 1 Lateralized decrease in brain volume per group per visit. Boxplots depicting brain volume (in mL) per group over time (visit 1 to 3) for study sample (n = 106). Red triangles flag mean volume, black strings the median. CON, healthy control; L, left; lv, logopenic variant; nfv, non-fluent variant; PPA, primary progressive aphasia; R, right; sv, semantic variant

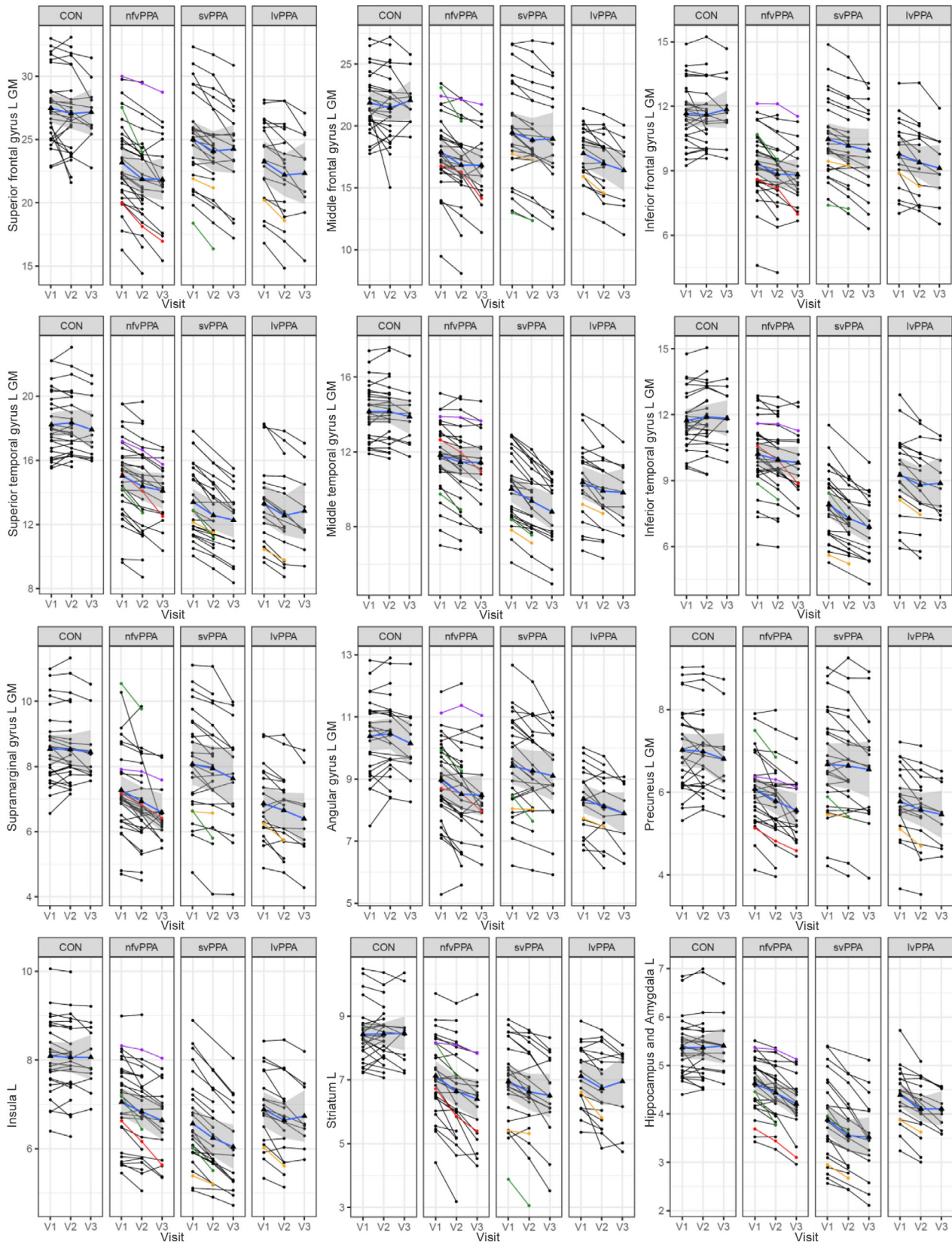


FIGURE 2 Individual trajectories of volume loss for distinct brain regions. Spaghetti plots depicting brain volume (in mL) development for distinctive regions per subject per group over time (visit 1 to 3) for study sample ($n = 106$). Dots mark factual examinations according to the FTLD protocol, the blue line depicts mean fitting per group with 95% confidence interval (gray shadow); C9orf72 mutation carrier (yellow); GRN mutation carrier (green); TBK1 mutation carrier (red); MAPT mutation carrier (purple). CON, healthy control; GM, gray matter; L, left; lv, logopenic variant; nfv, non-fluent variant; PPA, primary progressive aphasia; R, right; sv, semantic variant

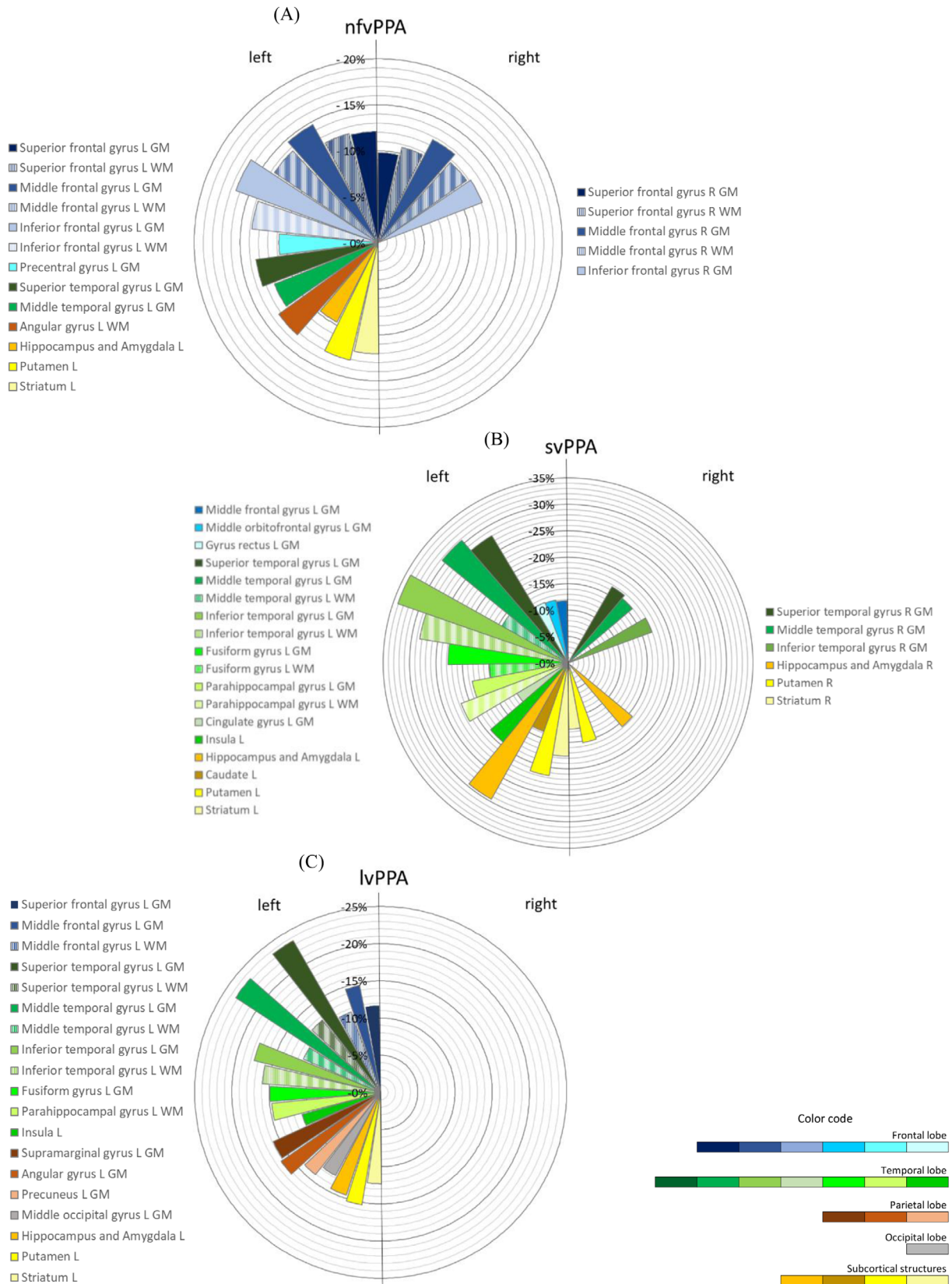


FIGURE 3 Volume difference between primary progressive aphasia (PPA) subgroup and healthy control (CON) at baseline. Cross-sectional comparison between CON and (A) non-fluent variant of primary progressive aphasia (nfvPPA), (B) semantic variant of primary progressive aphasia (svPPA), (C) logopenic variant of primary progressive aphasia (lvPPA) at baseline. All values were normalized to mean intracranial volume (ICV). Percentage difference to mean of healthy controls, values reported $P < .001$. R, right hemisphere; L, left hemisphere; GM, gray matter; WM, white matter

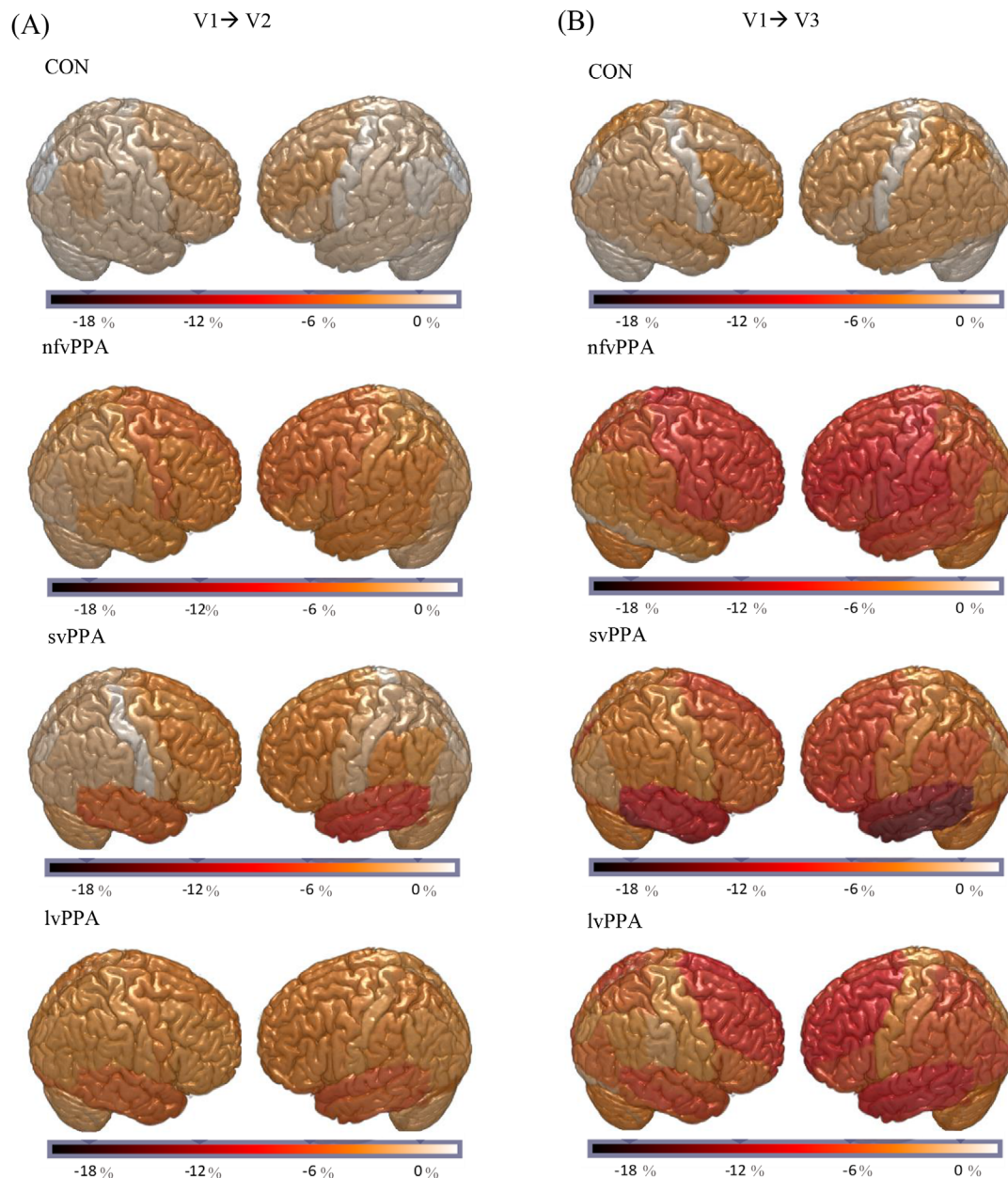


FIGURE 4 Longitudinal atrophy patterns in primary progressive aphasia (PPA) variants. Atrophy progression from baseline to (A) 1-year follow-up and (B) 2-year follow-up within each group. CON, healthy controls; lvPPA, logopenic variant of primary progressive aphasia; nfvPPA, non-fluent variant of primary progressive aphasia; svPPA, semantic variant of primary progressive aphasia

3.3.3 | Atrophy progression in lvPPA

The following regions differed in patients with lvPPA considerably ($P < .001$) from healthy controls over 1- and 2-year follow-up: Reduced volume was located in parts of the left frontal lobe, that is, in the superior (GM), middle (GM, WM) and inferior (GM) frontal gyrus, the lateral orbitofrontal (GM), and the precentral (GM) gyrus. Moreover, in the left temporal lobe, the superior (GM, WM), middle (GM, WM) and inferior (GM, WM) temporal gyrus, the parahippocampal (GM, WM), fusiform (GM, WM) and cingulate (GM) gyrus, as well as the left insula. Also, parts of the left parietal and left occipital lobe stand out

as deviant, in particular the postcentral (GM), superior parietal (GM), supramarginal (GM), angular (GM, WM), middle (GM) and inferior (GM) occipital gyrus, and the precuneus (GM). Significant right lateral volume deviation was located in the superior (GM) and middle (GM) frontal gyrus, the superior and middle temporal gyrus, and the middle occipital gyrus. On the subcortical level, the left striatum, bilateral putamen, and left hippocampus/amygdala complex differed most from healthy controls.

Results within the lvPPA group revealed highest atrophy rates (-6%) in the left superior and middle temporal gyrus (GM), the hippocampus/amygdala complex, and the left caudate (Figure 4A; Appendix S4).

Analyses from the 2-year follow-up rendered highest decline in the left hippocampus/amygdala complex (-11%) and in the left middle temporal gyrus (-10%; Figure 4B; Appendix S4).

3.4 | Sample size calculation for therapeutic trials

Based on mean atrophy rates for 1- and 2-year follow-up, we calculated sample sizes for a 50% to 10% treatment effect (Table 2), that is, a (50% to 10%) reduction in disease entailed volume decline. Despite various distributions, all three PPA subgroups showed some overlap so that a minimum sample size to predict therapeutic effects of 50%, 20%, and 10% in all groups over 1-year follow-up were found in the left temporal lobe GM ($n = 30,183,727$) and the left superior temporal gyrus GM ($n = 30,179,714$). Additionally, the left fusiform gyrus GM ($n = 27,159,630$), and the hippocampus/amygdala complex ($n = 26,157,626$) appeared sensitive to provide low sample sizes over 2-year follow-up for all variants. On a single group level, the left inferior frontal gyrus (GM), left superior temporal gyrus (GM), left striatum, and left caudate were the best indicators to control for therapeutic effects in *nfvPPA* 1-year follow-up. Beside the left superior, middle, and inferior temporal gyrus (GM), the hippocampus/amygdala complex, left insula, and the left fusiform gyrus (GM) appeared specifically sensitive for *svPPA*. Likewise, in *lvPPA* the left superior, middle, inferior temporal, and fusiform gyrus (GM) as well as the hippocampus/amygdala complex produced feasible estimates.

4 | DISCUSSION

This study aimed to examine atrophy progression in all three PPA subtypes with the help of MRI and automated ABV. Already at baseline, all PPA subgroups differed significantly from healthy controls with most pronounced volume reduction in the left ventrolateral prefrontal area for *nfvPPA*, the left temporal lobe, and hippocampus/amygdala complex for *svPPA*, and the left temporal and temporoparietal region for *lvPPA*. Follow-up measures over 1 and 2 year(s) revealed further atrophy progression in primarily affected areas in *nfvPPA* and *svPPA* and a more widespread pattern in *lvPPA*. In detailed regions, we found atrophy progression amounts above that reported in other studies.^{13,15,16,22-24} However, when observing greater entities such as the frontal or temporal lobe as a whole, rates were comparable. Especially in *svPPA* brain atrophy was more pronounced at baseline and in follow-up measures. First, this may be due to the fact that patients with *svPPA* are reported to contact medical care at later stages of the disease as symptoms appear insidious. Second, atrophy progression in *svPPA* occurs particularly limited to certain and primarily affected loci with restricted spreading, as our data imply. In contrast, in *lvPPA*, atrophy patterns at baseline and within 2-year follow-up represented more diffusely. Beside parietal and temporal atrophy noticeable tissue loss appeared in frontal regions. Lateral and medial frontal lobe involvement has been reported previously and was declared to occur within the course of disease progression throughout the entire language network.^{17,36-38} The pronounced frontal atrophy in our cohort

could be a consequence of the proportionately long disease duration (see Table 1).

Based on the standardized effect size of longitudinal volume decline we calculated sample sizes that slightly differ compared to the American study.²⁸ Methodologically, we also used an LME model to determine atrophy progression in PPA groups compared to healthy controls corrected for timepoint of measurement and stabilized for age and sex. However, we based our sample size calculation on effective volume decline as we present a fairly solid sample and consecutively conducted examinations exclusively. Differing sample size indications may be due to technical aspects assuming that ABV allows examining the whole brain in a more comprehensive manner. Moreover, as it becomes obvious in our longitudinal volume surveillance, the underlying neurodegenerative process progresses diffusely and may vary in stage of the disease, speed, and specific region per group, so that sample size indications may rely on varying origins and therapeutic trials should be planned to run for an extended period of time. Although the FTLD-CDR score provided (partially) lowest numbers for sample sizes, it is not meaningful in phrasing specific or discriminative statements and a certain risk of interrater variability and fluctuating scores in the range of individual disease courses complicate the review of disease progression and possible treatment effects. Therefore, MRI-based biomarkers are due to their rater-independency, accuracy, reliability, and particularly due to their specificity, an indispensable component when planning clinical trials and their outcome measures.

While this project tried to work out significant differences between PPA subgroups in comparison to healthy controls, we must mention that patterns of atrophy reflect a high degree of congruency underlining a common path of disease progression.

Although this is a comparably large follow-up study on patients with PPA, a limitation is the still small and unbalanced sample size. Moreover, assessing very small unities volumetrically may generate key figures that are more prone to over- or underestimation than those of larger compartments. Further studies considering a detailed analysis of the brain without a priori defined regions would be desirable. Methodologically, as the FTLD consortium study is still ongoing, we waived applying a longitudinal pipeline^{39,40} until all data sets per patient are available. However, current results justify confidence relating reconnaissance and implementation of potential therapies in all three PPA variants.

To conclude, our results show high atrophy rates both at baseline and for follow-up measures for all three PPA subgroups. Based on longitudinal volume change calculations, identified cohort sizes of $n = 30$ per variant prove a therapeutic effect of 50% within 1-year follow-up. With such a number per group double blind therapeutic trials promising a high effect are becoming feasible.

ACKNOWLEDGMENTS

We kindly thank all participants and their relatives for their participation as well as all coworkers of the FTLDc study group who enabled this project. This study was supported by the German Consortium for Frontotemporal Lobar Degeneration, funded by the German Federal Ministry of Education and Research (BMBF; grant no. FKZ01GI1007A), the

TABLE 2 Atrophy rates and sample size calculation for selected brain regions per PPA group

Region	Mean decline % (±SD)		Treatment effect					
	Baseline (V1) to 1-year follow-up	Baseline (V1) to 2-year follow-up	50% N		20% N		10% N	
	V1-2	V1-3	V1-2 (95% CI)	V1-3 (95% CI)	V1-2 (95% CI)	V1-3 (95% CI)	V1-2 (95% CI)	V1-3 (95% CI)
nfvPPA								
Cerebrum (WBV)	-3 (±2)	-6 (±4)	65 (40-133)	45 (25-115)	396 (243-824)	275 (153-727)	1580 (968-3297)	1097 (609-2887)
Frontal lobe R	-4 (±4)	-7 (±5)	158 (77-539)	76 (40-323)	978 (470-3365)	467 (244-2109)	3906 (1875-10,000+)	1863 (973-8451)
Frontal lobe L	-4 (±4)	-8 (±6)	84 (50-163)	49 (28-113)	518 (307-1072)	299 (171-727)	2068 (1226-4330)	1191 (683-2904)
Temporal lobe R	-2 (±2)	-4 (±6)	69 (38-169)	154 (22-10,000+)	422 (229-1051)	954 (128-10,000+)	1684 (916-4202)	3811 (507-10,000+)
Temporal lobe L	-3 (±3)	-7 (±4)	45 (28-85)	23 (12-54)	271 (164-523)	135 (66-330)	1079 (653-2090)	535 (260-1315)
Frontal lobe L GM	-5 (±4)	-9 (±6)	48 (31-76)	32 (18-59)	295 (191-474)	192 (108-362)	1177 (764-1917)	762 (425-1444)
Temporal lobe L GM	-3 (±3)	-7 (±5)	30 (18-47)	27 (15-54)	183 (114-315)	160 (84-329)	727 (453-1257)	637 (337-1318)
Inferior frontal gyrus L GM	-5 (±4)	-8 (±6)	45 (28-85)	36 (21-106)	273 (170-544)	219 (131-1145)	1087 (676-2181)	873 (524-4809)
Superior temporal gyrus L GM	-4 (±4)	-8 (±5)	30 (17-52)	29 (15-84)	179 (106-332)	173 (88-529)	714 (422-1335)	688 (348-2115)
Striatum L	-7 (±7)	-11 (±8)	48 (29-83)	34 (18-77)	290 (171-514)	206 (107-486)	1156 (681-2052)	819 (422-1943)
Caudate L	-7 (±8)	-12 (±10)	49 (30-88)	36 (20-78)	301 (187-574)	216 (116-479)	1199 (741-2294)	858 (459-1912)
MIMSE (points)	-3 (±4)	-8 (±6)	65 (28-275)	25 (11-62)	400 (167-1730)	149 (64-389)	1596 (665-6912)	593 (253-1558)
FTLD-CDR (points)	2 (±2)	4 (±3)	32 (17-53)	22 (10-51)	192 (98-321)	131 (63-337)	762 (387-1278)	518 (250-1344)
svPPA								
Cerebrum (WBV)	-3 (±2)	-5 (±3)	49 (30-86)	45 (24-196)	299 (182-536)	271 (143-838)	1191 (721-2138)	1080 (524-3366)
Frontal lobe R	-3 (±3)	-4 (±4)	347 (116-6244)	501 (115-10,000+)	2162 (716-10,000+)	3126 (706-10,000+)	8642 (2862-10,000+)	12501 (2822-10,000+)
Frontal lobe L	-3 (±3)	-6 (±4)	138 (60-563)	92 (39-427)	853 (368-3520)	565 (236-2660)	3408 (1467-10,000+)	2255 (937-10,000+)
Temporal lobe R	-5 (±2)	-9 (±4)	12 (9-15)	11 (6-21)	67 (52-90)	61 (32-133)	262 (204-357)	240 (124-537)
Temporal lobe L	-7 (±3)	-11 (±4)	8 (6-9)	7 (4-14)	45 (34-65)	39 (19-126)	177 (134-269)	150 (70-468)

(Continues)

TABLE 2 (Continued)

Region	Mean decline % (±SD) Baseline (V1) to 1-year follow-up V1-2	Baseline (V1) to 2-year follow-up V1-3	Treatment effect					
			50% N		20% N		10% N	
			V1-2 (95% CI)	V1-3 (95% CI)	V1-2 (95% CI)	V1-3 (95% CI)	V1-2 (95% CI)	V1-3 (95% CI)
Temporal lobe L GM	-7 (±3)	-13 (±5)	8 (6-10)	7 (3-15)	43 (31-63)	38 (17-144)	167 (124-251)	148 (65-827)
Insula L	-6 (±2)	-10 (±4)	11 (8-16)	11 (4-32)	59 (41-95)	16 (19-205)	232 (164-389)	236 (73-814)
Superior temporal gyrus L GM	-7 (±3)	-12 (±5)	11 (8-19)	11 (5-32)	59 (41-110)	61 (23-230)	233 (162-456)	240 (90-915)
Middle temporal gyrus L GM	-8 (±4)	-15 (±6)	11 (7-17)	9 (5-24)	59 (36-97)	46 (21-139)	232 (142-384)	178 (80-547)
Inferior temporal gyrus L GM	-8 (±4)	-15 (±6)	10 (7-14)	8 (4-16)	56 (40-90)	45 (23-135)	219 (156-360)	175 (86-538)
Fusiform gyrus L GM	-7 (±3)	-13 (±4)	14 (10-18)	6 (3-11)	80 (61-113)	29 (14-71)	315 (238-446)	130 (57-296)
Hippocampus & Amygdala	-8 (±2)	-13 (±6)	9 (7-9)	10 (5-18)	51 (42-63)	57 (30-131)	200 (165-253)	225 (116-520)
MMSE (points)	-3 (±5)	-3 (±3)	89 (35-457)	43 (16-260)	550 (209-2847)	262 (94-1614)	2196 (829-10,000+)	1045 (371-6724)
FTLD-CDR (points)	2 (±2)	3 (±3)	41 (19-76)	31 (13-99)	249 (109-467)	184 (76-664)	992 (433-1863)	732 (306-2653)
IVPPA								
Cerebrum (WBV)	-3 (±2)	-5 (±3)	51 (28-110)	35 (16-112)	309 (167-677)	213 (95-737)	1231 (665-2704)	847 (376-2949)
Frontal lobe R	-2 (±3)	-6 (±4)	818 (158-10,000+)	126 (31-10,000+)	5105 (978-10,000+)	779 (188-10,000+)	20414 (3909-10,000+)	3110 (746-10,000+)
Frontal lobe L	-3 (±2)	-7 (±3)	231 (81-1299)	40 (18-124)	1433 (495-8108)	242 (105-841)	5729 (1976-10,000+)	964 (418-3360)
Temporal lobe R	-4 (±3)	-5 (±3)	30 (17-144)	25 (10-2391)	182 (101-1045)	148 (58-10,000+)	723 (399-4198)	589 (229-10,000+)
Temporal lobe L	-5 (±2)	-8 (±4)	15 (10-34)	11 (5-98)	85 (55-205)	59 (23-603)	336 (216-820)	232 (87-2408)
Superior temporal gyrus L GM	-6 (±3)	-9 (±4)	13 (8-22)	10 (5-24)	73 (44-139)	56 (28-174)	289 (178-567)	218 (108-688)
Middle temporal gyrus L GM	-5 (±4)	-10 (±5)	24 (14-63)	15 (5-63)	145 (81-413)	88 (28-442)	575 (319-1645)	349 (108-1805)
Inferior temporal gyrus L GM	-6 (±4)	-8 (±6)	17 (10-41)	21 (10-296)	98 (59-275)	125 (53-2087)	389 (232-1165)	497 (241-9647)
Fusiform gyrus L GM	-5 (±4)	-7 (±5)	27 (17-46)	16 (8-49)	163 (106-307)	93 (42-332)	647 (423-1223)	367 (164-1328)
Hippocampus & Amygdala	-6 (±5)	-9 (±4)	26 (16-48)	11 (6-32)	155 (77-266)	60 (30-213)	616 (306-1069)	236 (120-871)
MMSE (points)	-3 (±4)	-6 (±5)	77 (26-3238)	26 (8-3047)	472 (162-10,000+)	153 (43-10,000+)	1882 (642-10,000+)	609 (167-10,000+)
FTLD-CDR (points)	3 (±2)	+3 (±2)	9 (4-13)	18 (5-88)	48 (21-84)	104 (28-568)	186 (81-332)	411 (109-2264)

Abbreviations: FTLD-CDR, Frontotemporal-specific Clinical Dementia Rating; GM, gray matter; L, left; MMSE, Mini-Mental State Examination; R, right; WBV, whole brain volume.
Note: Sample size calculation for a 50% to 10% treatment effect based on the mean atrophy rate per group per brain region within 1-/2-year follow-up (baseline to V2 [V1-2] or baseline to V3 [V1-3]).

EU Joint Programme—Neurodegenerative Disease Research (JPND) network (project: SOPHIA, BiomarkAPD), PreFrontAIs (BMBF; grant no. 01ED1512), the foundation of the state of Baden-Württemberg (D.3830), BIU (D.5009), the EU's Horizon 2020 framework programme (Fairpark II). MLS also has been supported by the [German Research Foundation](#) (DFG; SCHR 774/5-1).

Open access funding enabled and organized by Projekt DEAL.

HUMAN ETHICS APPROVAL DECLARATION

The study was approved by the local ethics committees (proposal number at the central study center at University of Ulm, 39/11, 8 March 2011). On-site monitoring was conducted regularly for all patient data. Every participant or his/her legal representative, respectively, signed written informed consent.

CONFLICTS OF INTEREST

The authors report no competing interests.

AUTHOR CONTRIBUTIONS

Data acquisition: Jolina Lombardi, Elisa Semler, Sarah Anderl-Straub, Ingo Uttner, Janine Diehl-Schmid, Adrian Danek, Johannes Levin, Klaus Fassbender, Klaus Fliessbach, Anja Schneider, Holger Jahn, Johannes Kornhuber, Martin Lauer, Johannes Prudlo, Jens Wiltfang, Matthias L. Schroeter, Markus Otto. Study concept and design: Sarah Anderl-Straub, Ingo Uttner, Janine Diehl-Schmid, Adrian Danek, Johannes Levin, Klaus Fassbender, Klaus Fliessbach, Anja Schneider, Holger Jahn, Johannes Kornhuber, Bernhard Landwehrmeyer, Martin Lauer, Johannes Prudlo, Jens Wiltfang, Matthias L. Schroeter, Albert Ludolph, Markus Otto. Analysis and interpretation of data: Jolina Lombardi, Benjamin Mayer, Elisa Semler, Sarah Anderl-Straub, Jan Kassubek, Hans-Jürgen Huppertz, Alexander Volk, Markus Otto. Drafting of the manuscript: Jolina Lombardi, Benjamin Mayer, Markus Otto. Critical revision of the manuscript for important intellectual content: Benjamin Mayer, Ingo Uttner, Jan Kassubek, Janine Diehl-Schmid, Hans-Jürgen Huppertz, Matthias L. Schroeter, Markus Otto. Statistical analysis: Jolina Lombardi, Benjamin Mayer.

DATA AVAILABILITY STATEMENT

The data that support the findings of this study are available from the corresponding author upon reasonable request.

REFERENCES

- Mesulam MM. Primary progressive aphasia. *Ann Neurol*. 2001;49:425-432.
- Gorno-Tempini ML, Hillis AE, Weintraub S, et al. Classification of primary progressive aphasia and its variants. *Neurology*. 2011;76(11):1006-1014.
- Mesulam MM, Wieneke C, Thompson C, Rogalski E, Weintraub S. Quantitative classification of primary progressive aphasia at early and mild impairment stages. *Brain*. 2012;135(5):1537-1553.
- Gorno-Tempini ML, Dronkers NF, Rankin KP, et al. Cognition and anatomy in three variants of primary progressive aphasia. *Ann Neurol*. 2004;55(3):335-346.
- Wilson SM, Galantucci S, Tartaglia MC, Gorno-Tempini ML. The neural basis of syntactic deficits in primary progressive aphasia. *Brain Lang*. 2012;122(3):190-198.
- Mesulam MM, Rogalski E, Wieneke C, et al. Primary progressive aphasia and the evolving neurology of the language network. *Sci*. 2008;75(1):154-161.
- Bisenius S, Mueller K, Diehl-Schmid J, et al. Schroeter, & FtlD study group: predicting primary progressive aphasias with support vector machine approaches in structural MRI data. *NeuroImage Clin*. 2017;14:334-343.
- Bisenius S, Neumann J, Schroeter ML. Validating new diagnostic imaging criteria for primary progressive aphasia via anatomical likelihood estimation meta-analyses. *Eur J Neurol*. 2016;23(4):704-712.
- Schroeter ML, Raczkka K, Neumann J, Yves von Cramon D. Towards a nosology for frontotemporal lobar degenerations—a meta-analysis involving 267 subjects. *Neuroimage*. 2007;36(3):497-510.
- Chan D, Fox NC, Scahill RI, et al. Patterns of temporal lobe atrophy in semantic dementia and Alzheimer's disease. *Ann Neurol*. 2001;49(4):433-442.
- Mummery CJ, Patterson K, Price CJ, Ashburner J, Frackowiak RSJ, Hodges JR. A voxel-based morphometry study of semantic dementia: relationship between temporal lobe atrophy and semantic memory. *Ann Neurol*. 2000;47(1):36-45.
- Whitwell JL, Anderson VM, Scahill RI, Rossor MN, Fox NC. Longitudinal patterns of regional change on volumetric MRI in frontotemporal lobar degeneration. *Dement Geriatr Cogn Disord*. 2004;17(4):307-310.
- Krueger CE, Dean DL, Rosen HJ, Halabi C, Miller BL, Kramer JH. Longitudinal rates of lobar atrophy in frontotemporal dementia, semantic dementia, and Alzheimer's disease. *Alzheimer Dis Assoc Disord*. 2010;24(1):43-48.
- Rogalski E, Cobia D, Harrison TM, Wieneke C, Weintraub S, Mesulam MM. Progression of language decline and cortical atrophy in subtypes of primary progressive aphasia. *Neurology*. 2011;76(21):1804-1810.
- Frings L, Mader I, Landwehrmeyer BG, Weiller C, Hüll M, Huppertz HJ. Quantifying change in individual subjects affected by frontotemporal lobar degeneration using automated longitudinal MRI volumetry. *Hum Brain Mapp*. 2012;33(7):1526-1535.
- Rohrer JD, Clarkson MJ, Kittur R, et al. Rates of hemispheric and lobar atrophy in the language variants of frontotemporal lobar degeneration. *J Alzheimer's Dis*. 2012;30(2):407-411.
- Rohrer JD, Caso F, Mahoney C, et al. Patterns of longitudinal brain atrophy in the logopenic variant of primary progressive aphasia. *Brain Lang*. 2013;127(2):121-126.
- Lu PH, Mendez MF, Lee GJ, et al. Patterns of brain atrophy in clinical variants of frontotemporal lobar degeneration. *Dement Geriatr Cogn Disord*. 2013;35(1-2):34-50.
- Rogalski E, Cobia D, Martnersteck A, et al. Asymmetry of cortical decline in subtypes of primary progressive aphasia. *Neurology*. 2014;83(13):1184-1191.
- Seeley WW, Crawford RK, Zhou J, Miller BL, Greicius MD. Neurodegenerative diseases target large-scale human brain networks. *Neuron*. 2009;62(1):42-52.
- Chan D, Fox NC, Jenkins R, Scahill RI, Crum WR, Rossor MN. Rates of global and regional cerebral atrophy in AD and frontotemporal dementia. *Neurology*. 2001;57(10):1756-1763.
- Rohrer JD, McNaught E, Foster J, et al. Tracking progression in frontotemporal lobar degeneration: serial MRI in semantic dementia. *Neurology*. 2008;71(18):1445-1451.
- Knopman DS, Jack CR, Kramer JH, et al. Brain and ventricular volumetric changes in frontotemporal lobar degeneration over 1 year. *Neurology*. 2009;72(21):1843-1849.
- Gordon E, Rohrer JD, Kim LG, et al. Measuring disease progression in frontotemporal lobar degeneration: a clinical and MRI study. *Neurology*. 2010;74(8):666-673.
- Fotenos AF, Snyder AZ, Girton LE, Morris JC, Buckner RL. Normative estimates of cross-sectional and longitudinal brain volume decline in aging and AD. *Neurology*. 2005;64(6):1032-1039.

26. Resnick SM, Pham DL, Kraut MA, Zonderman AB, Davatzikos C. Longitudinal magnetic resonance imaging studies of older adults: a shrinking brain. *J Neurosci*. 2003;23(8):3295-3301.
27. Fjell AM, Walhovd KB, Fennema-Notestine C, et al. One-year brain atrophy evident in healthy aging. *J Neurosci*. 2009;29(48):15223-15231.
28. Staffaroni AM, Ljubenkov PA, Kornak J, et al. Longitudinal multimodal imaging and clinical endpoints for frontotemporal dementia clinical trials. *Brain*. 2019;142(2):443-459.
29. Semler E, Anderl-Straub S, Uttner I, et al. A language-based sum score for the course and therapeutic intervention in primary progressive aphasia. *Alzheimer's Res Ther*. 2018;10(1):1-10.
30. Steinacker P, Semler E, Anderl-Straub S, et al. Neurofilament as a blood marker for diagnosis and monitoring of primary progressive aphasias. *Neurology*. 2017;88(10):961-969.
31. Knopman DS, Kramer JH, Boeve BF, et al. Development of methodology for conducting clinical trials in frontotemporal lobar degeneration. *Brain*. 2008;131(11):2957-2968.
32. Shattuck David W., Mirza Mubeena, Adisetiyo Vitria, Hojatkashani Cornelius, Salamon Georges, Narr Katherine L., Poldrack Russell A., Bilder Robert M., Toga Arthur W. (2008) Construction of a 3D probabilistic atlas of human cortical structures. *NeuroImage*, 39 (3), 1064–1080. <http://doi.org/10.1016/j.neuroimage.2007.09.031>.
33. Huppertz HJ, Kröll-Seger J, Klöppel S, Ganz RE, Kassubek J. Intra- and interscanner variability of automated voxel-based volumetry based on a 3D probabilistic atlas of human cerebral structures. *Neuroimage*. 2010;49(3):2216-2224.
34. Bernal-Rusiel JL, Greve DN, Reuter M, Fischl B, Sabuncu MR. Statistical analysis of longitudinal neuroimage data with Linear Mixed Effects models. *Neuroimage*. 2013;66:249-260.
35. Müller HP, Huppertz HJ, Dreyhaupt J, et al. Combined cerebral atrophy score in Huntington's disease based on atlas-based MRI volumetry: sample size calculations for clinical trials. *Park Relat Disord*. 2019;63(December 2018):179-184.
36. Madhavan A, Whitwell JL, Weigand SD, et al. FDG PET and MRI in logopenic primary progressive aphasia versus dementia of the Alzheimer's type. *PLoS One*. 2013;8(4):1-9.
37. Teichmann M, Kas A, Boutet C, et al. Deciphering logopenic primary progressive aphasia: a clinical, imaging and biomarker investigation. *Brain*. 2013;136(11):3474-3488.
38. Preiß D, Billette OV, Schneider A, Spotorno N, Nestor PJ. The atrophy pattern in Alzheimer-related PPA is more widespread than that of the frontotemporal lobar degeneration associated variants. *NeuroImage Clin*. 2019;24(July):101994.
39. Ashburner J, Ridgway GR. Symmetric diffeomorphic modeling of longitudinal structural MRI. *Front Neurosci*. 2013;6(FEB):1-19.
40. Cash DM, Frost C, Iheme LO, et al. Assessing atrophy measurement techniques in dementia: results from the MIRIAD atrophy challenge. *Neuroimage*. 2015;123:149-164.

SUPPORTING INFORMATION

Additional supporting information may be found online in the Supporting Information section at the end of the article.

How to cite this article: Lombardi J, Mayer B, Semler E, et al. Quantifying progression in primary progressive aphasia with structural neuroimaging. *Alzheimer's Dement*. 2021;1-15. <https://doi.org/10.1002/alz.12323>